Supplementary Information (SI) for Nanoscale.

Supporting Information

Unrevealing the Activity Promotion of the Hierarchical Yolk-Shell Structure Based on Co-Glycerate@Cobalt Carbonate Hydroxide by Dual Doping of the Manganese and Boron for Prompt Tri-functional ORR, OER, and HER

Maryam Shamloofard, Saeed Shahrokhian*

Department of Chemistry, Sharif University of Technology, Tehran 11155-9516, Iran

Electrochemical investigations

The linear sweep voltammetry (LSV), cyclic voltammetry (CV), electrochemical impedance spectroscopy (EIS) and chronoamperometry were investigated at room temperature using an electrochemical workstation (Autolab 204) for monitoring the electrochemical performance of the catalysts toward OER, HER and ORR. The electrochemical performances were tested in three-electrode configuration including Hg/HgO as a reference electrode, a graphite rod as a counter electrode and the graphite papers (0.5 cm × 1 cm) modified with the prepared catalysts as a working electrode for OER and HER. For ORR investigation, the working electrode was the modified rotating disk electrode (RDE) with 3.5-mm-diameter. In order to modification of the rotating disk electrode as a working electrode for ORR, the amounts of 5 mg prepared catalysts were dissolved 1mL of 3:1 (v/v) water/ethanol with 10 μL of a 5 wt % Nafion and then 5 μL of the prepared homogenous suspensions were loaded on the surface of the RDE. An alkaline solution (1.0 M KOH) with pH = 14 was employed as the electrolyte for OER and HER and the 0.1 M KOH was used as the electrolyte for ORR. In the ORR monitoring, the alkaline solution of 0.1 M KOH was saturated with O_2 gas for least 30 min before each experiment. In order to prepare the working electrodes for OER and HER, first, the graphite papers were placed in ethanol and acetone for ten minutes to remove impurities on the surface of them. Subsequently, 5 mg of the prepared catalysts were dispersed into a mixture solution including 10 μL of a 5 wt % Nafion and 1mL of 3:1 (v/v) water/ethanol. After that, the working electrodes were fabricated by loading 5 μL of the homogenous suspension on the surface of the graphite paper. Prior to the measurements, the working electrodes were pretreated in 1.0 M KOH electrolyte via cyclic voltammetry for 15 cycles in the potential window from 0.2 to 0.6 V (vs. Hg/HgO) with a scan rate of 50 mV s^{-1} until the CV curves become stable. In ORR investigation, the CVs were performed in Ar and O_2 saturated electrolyte with a scan rate of 50 mV s^{-1} and the LSVs were evaluated with a scan rate of 5 mV s^{-1} in O_2 saturated electrolyte at 200, 600, 1200, 1600, 2000 and 2400 rpm. The polarization curves were obtained by linear sweep voltammetry (LSV) measurements at a scan rate of 5 mV s^{-1} in the potential range of 1.2 to 1.8 V (vs. RHE) for OER, 0.2 to -0.7 V (vs. RHE) for HER, and 1.1 to 0 (vs. RHE) V (vs. RHE) for ORR. All the measurement potentials were corrected throughout the system for IR-drop and calibrated to the reversible hydrogen electrode (RHE). The relationship between Hg/HgO electrode potentials and RHE potentials based on the Nernst equation is:[1,2]

$$E_{RHE} = E_{Hg/HgO} + E^{\circ}_{Hg/HgO} + 0.059\ pH\ (V) \qquad (1)$$

Also, the RuO_2 and Pt/C (20 wt%) as the benchmark catalysts for OER and HER, respectively, were used to comparison with other synthesized catalysts. For preparation of the RuO_2/GP and Pt/C/GP electrodes, 5 mg of the RuO_2 and Pt/C (20 wt%) were added to a mixture solution including 10 μL of a 5 wt % Nafion and 1mL of 3:1 (v/v) water/ethanol. Then, 5 μL of the homogenous suspensions were loaded on the graphite paper surface to prepare the RuO_2/GP and Pt/C/GP electrodes.

The Nyquist plots were investigsted at 1.0 M KOH by electrochemical impedance spectroscopy (EIS) measurements at the ac voltage of 5 mV and the the frequency range of 0.1 Hz to 10 kHz. The bias voltage for the OER and HER was 0.5 V (vs. Ag/AgCl) and −1.1 V (vs. Ag/AgCl), repectively.

Also, the electron transfer numbers were obtained based on the Koutecky−Levich equations:[3]

$$1/j = 1/j_k + 1/j_L = 1/j_k + 1/(B\omega^{1/2}) \quad (2)$$

$$B = 0.62nFC_0(D_0)^{2/3}\, v^{1/6} \quad (3)$$

The j, j_k and j_L are the measured current density, the kinetic current density, and the diffusion-limited current density, respectively, ω is the angular velocity, F is the Faraday constant (F = 96485 C mol^{-1}), C_0 is the concentration of bulk O_2 with the amount of 1.2×10^{-6} mol cm^{-3}, D_0 is the diffusion coefficient of O_2 with the amount of 1.9×10^{-5} cm^2 s^{-1} and v is the kinetic viscosity (0.01 cm^2 s^{-1}).

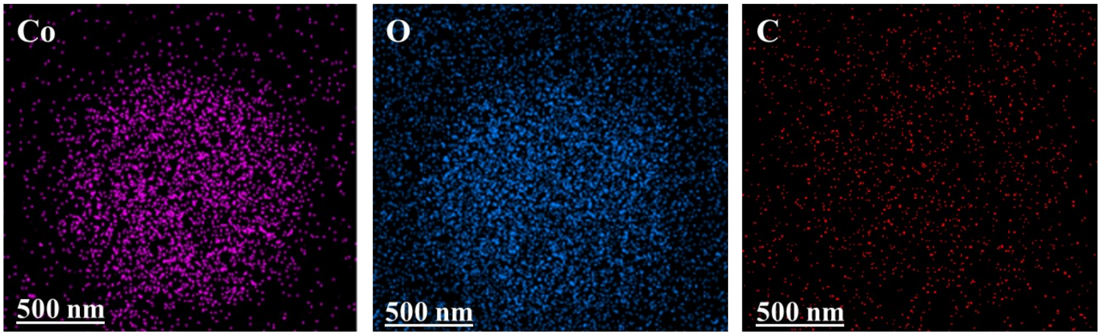

Figure S1. Elemental mapping analysis of the CoG

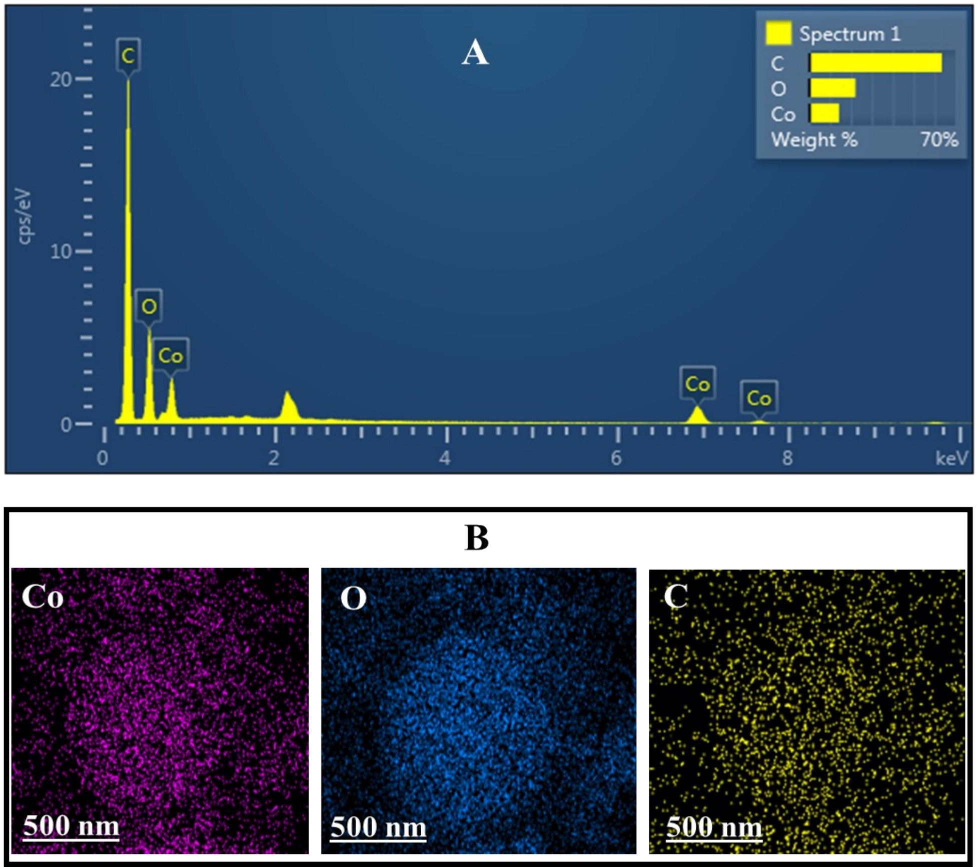

Figure S2. (A) Energy-dispersive X-ray, (B) Elemental mapping analysis of the CoGSS@CoCHNs

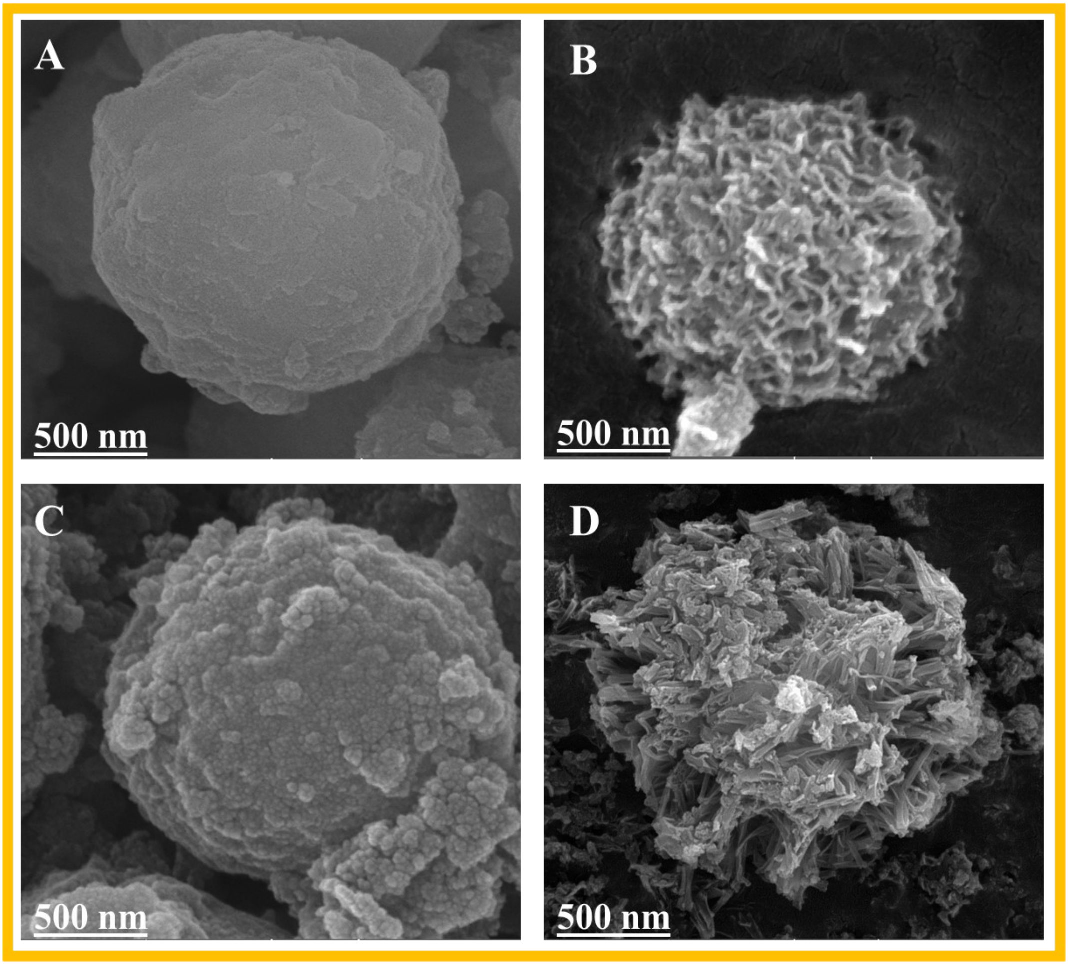

Figure S3. The FE-SEM images of **(A)** $Mn_{(0.02)}$-CoGSS@CoCHNs, **(B)** $Mn_{(0.04)}$-CoGSS@CoCHNs, **(C)** $Mn_{(0.08)}$-CoGSS@CoCHNs **(D)** $Mn_{(0.12)}$-CoGSS@CoCHNs.

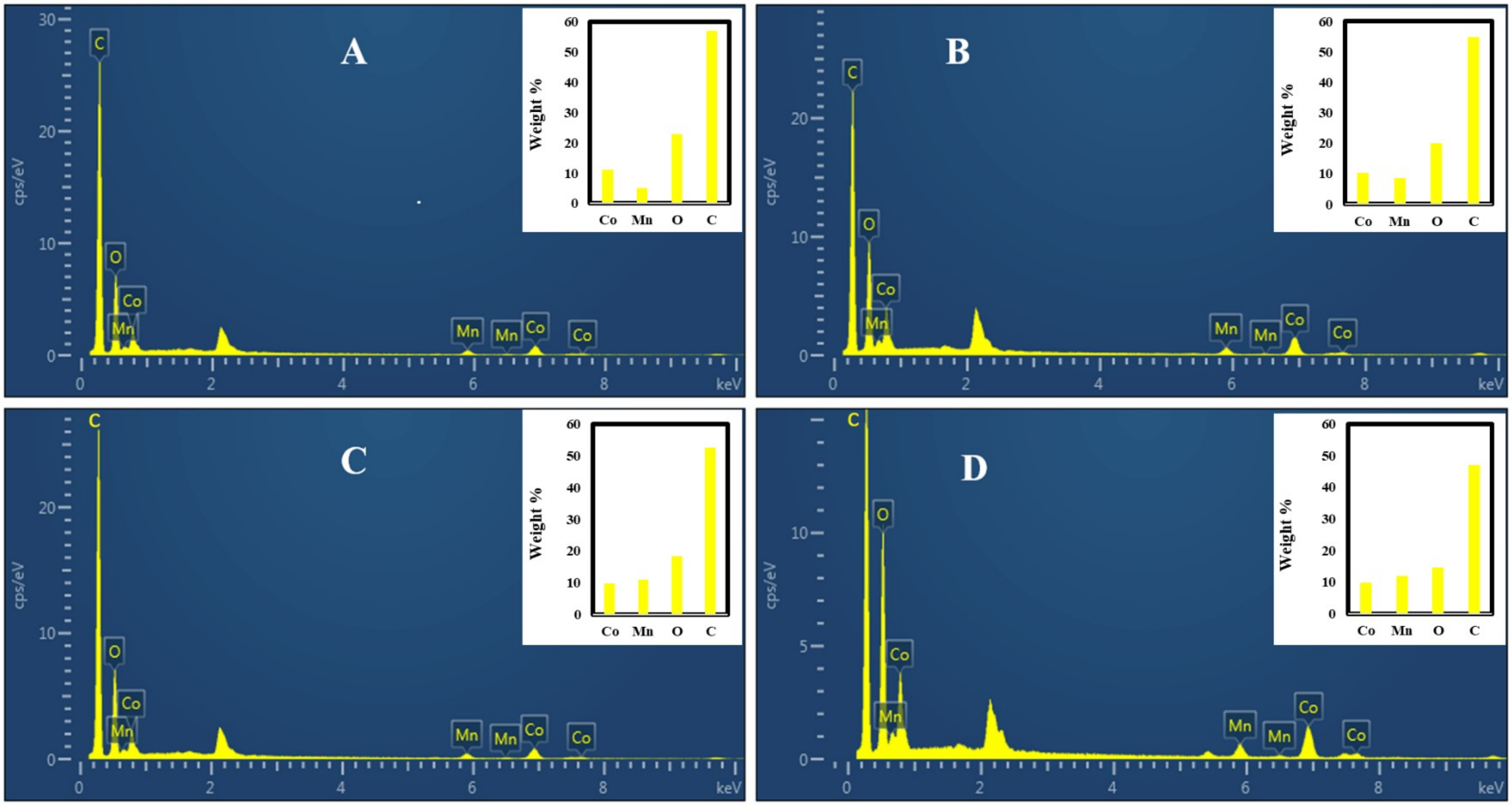

Figure S4. Energy-dispersive X-ray of the **(A)** Mn$_{(0.02)}$-CoGSS@CoCHNs, **(B)** Mn$_{(0.04)}$-CoGSS@CoCHNs, **(C)** Mn$_{(0.08)}$-CoGSS@CoCHNs **(D)** Mn$_{(0.12)}$-CoGSS@CoCHNs.

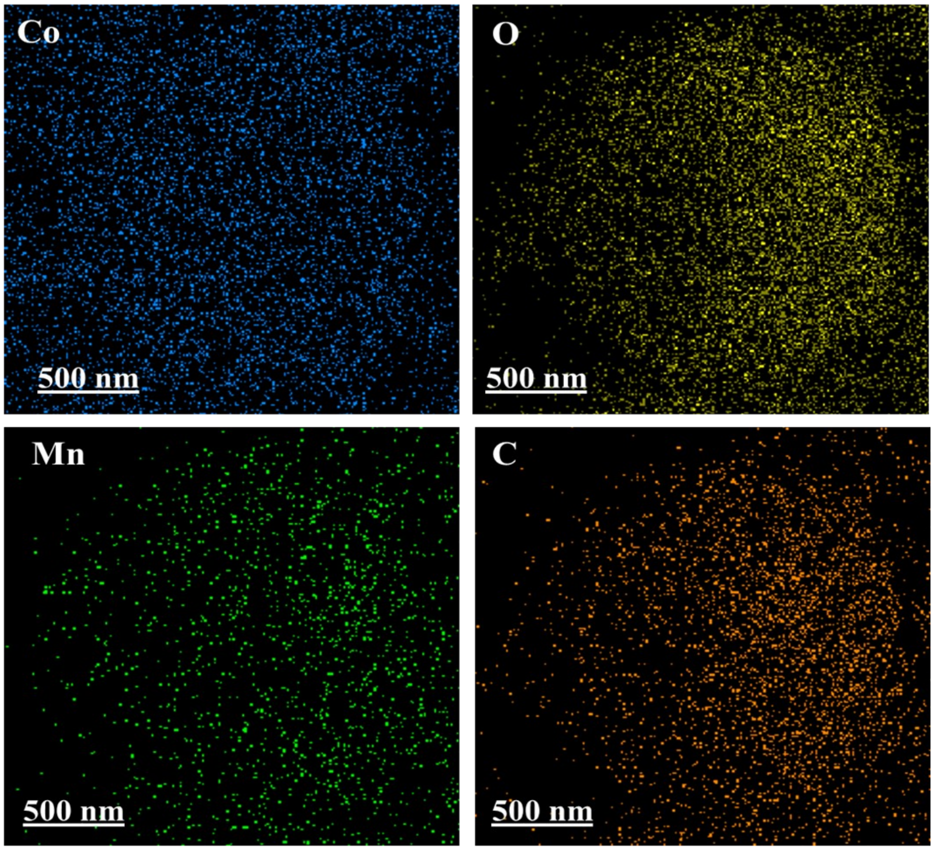

Figure S5. Elemental mapping analysis of the $Mn_{(0.04)}$-CoGSS@CoCHNs

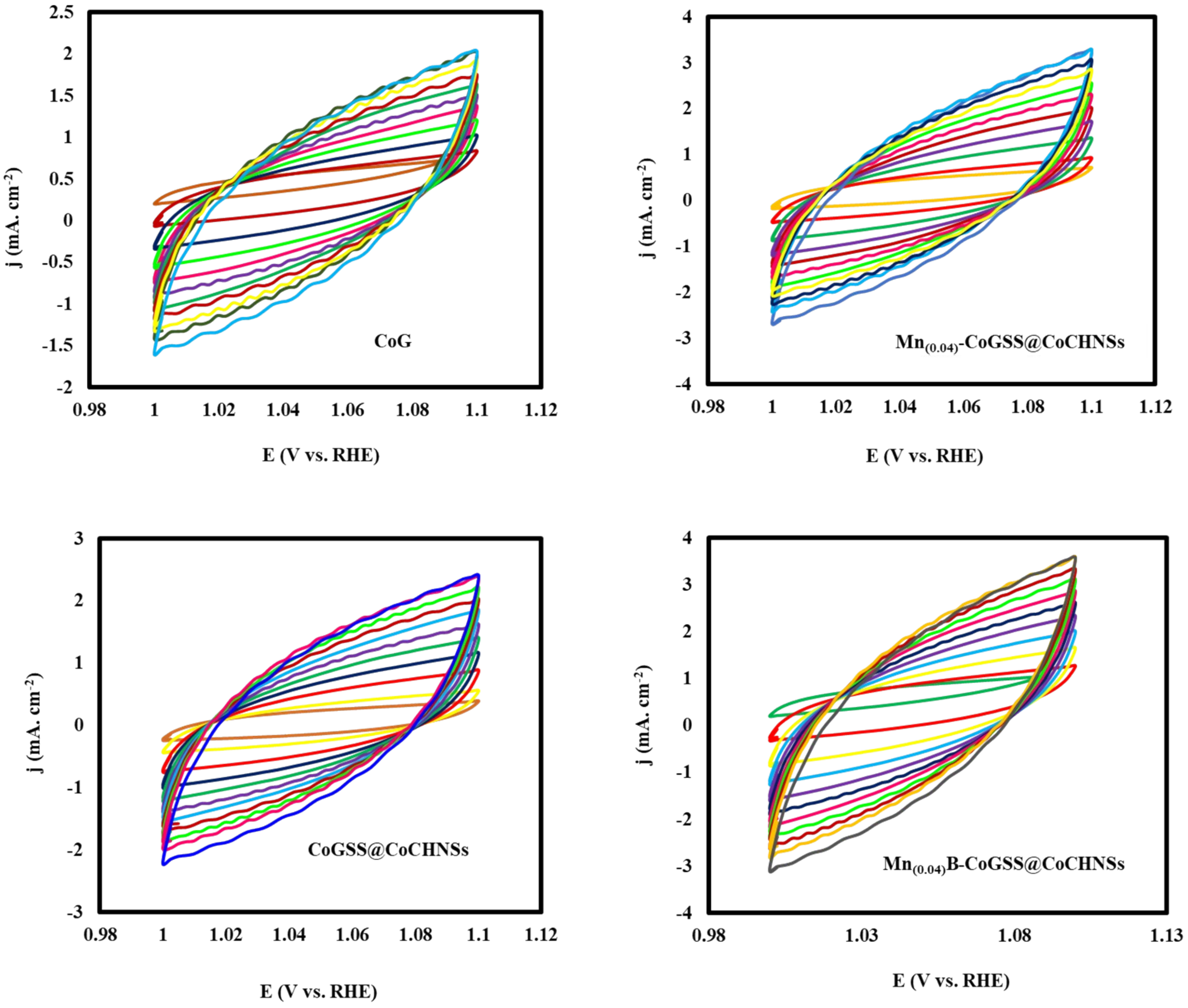

Figure S6. CV curves of catalysts in 1M KOH with different scan rates (5-100 mV s^{-1})

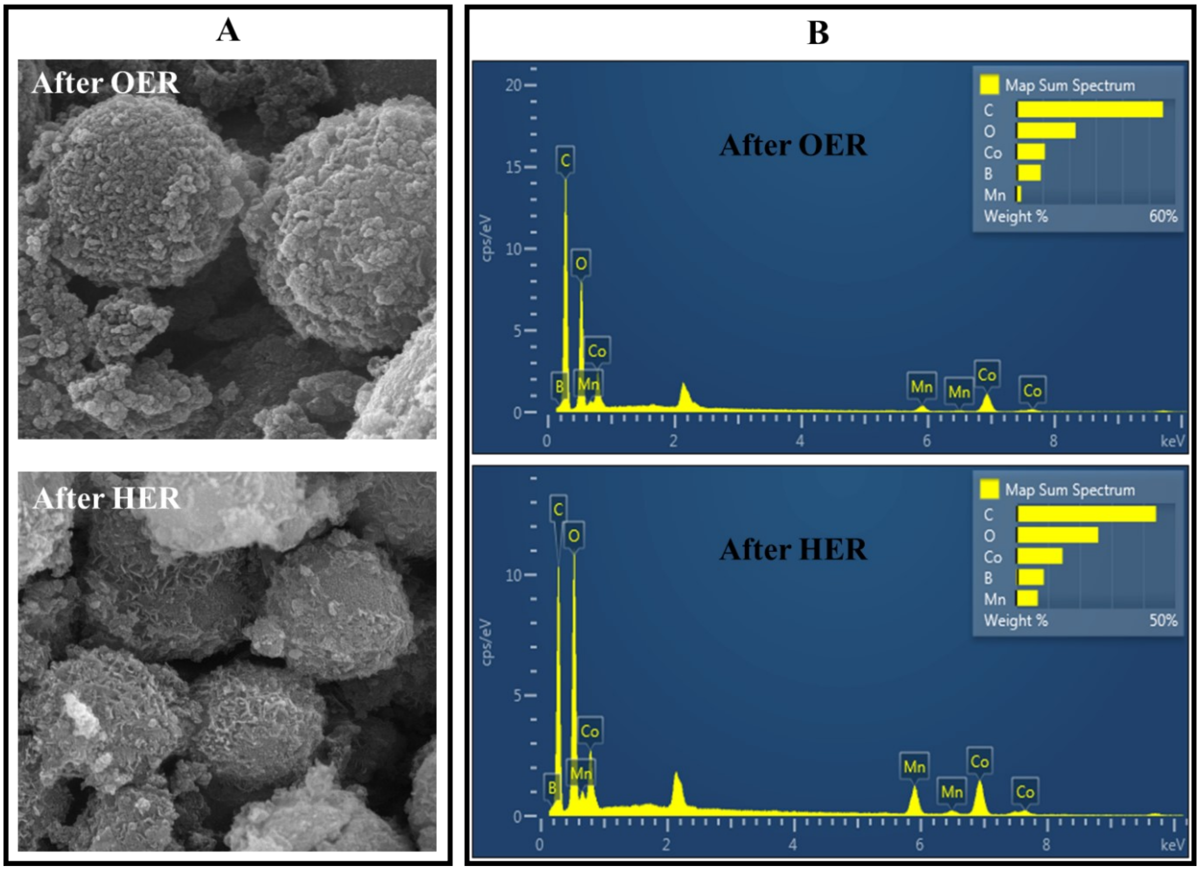

Figure S7. (A) The FE-SEM images, and **(B)** Energy-dispersive X-ray of the Mn$_{(0.04)}$B-CoGSS@CoCHNs after OER and HER tests.

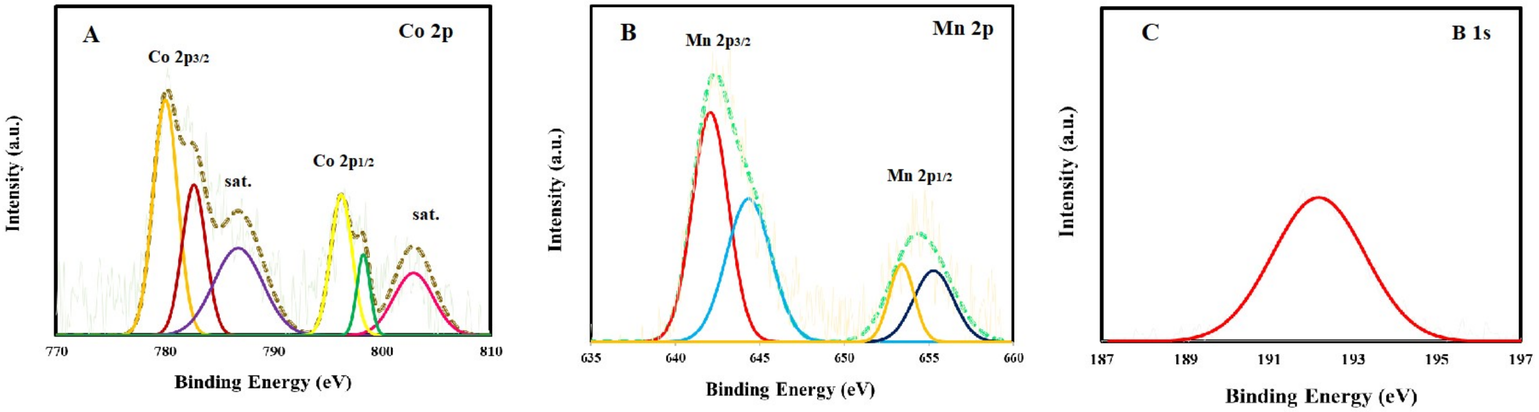

Figure S8. XPS of the $Mn_{(0.04)}$B-CoGSS@CoCHNSs catalyst after OER.

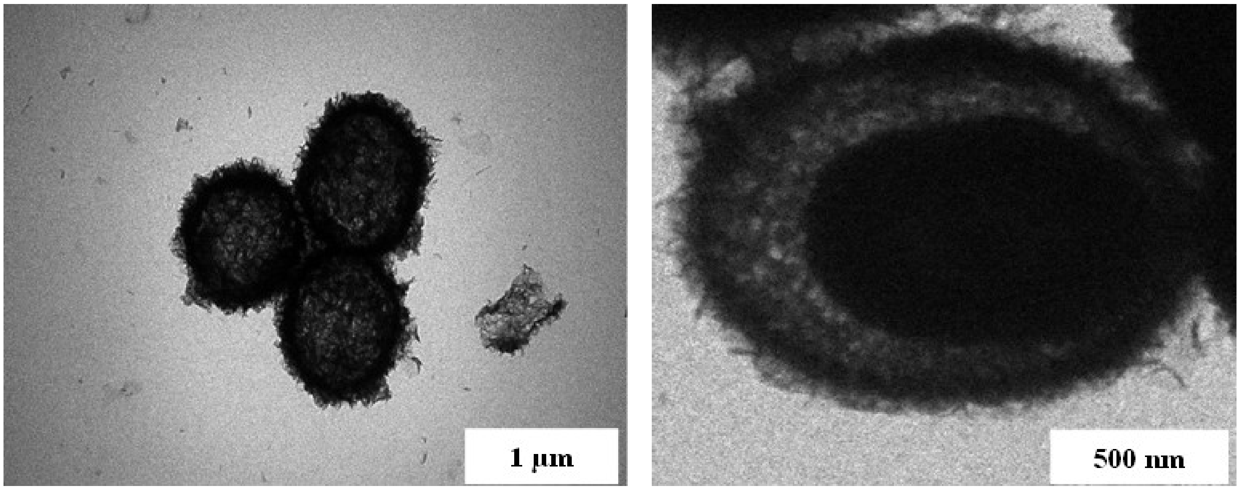

Figure S9. TEM of the $Mn_{(0.04)}$B-CoGSS@CoCHNSs catalyst after OER.

Table S1. Comparison of the TOF and ECSA of the catalysts.

Catalysts	**ECSA (m^2/g)**	**TOF (ORR) s^{-1} at the 0.9 V**
CoGSS	**23.1**	**1.16**
CoGSS@CoCHNSs	**40.8**	**1.58**
$Mn_{(0.04)}$-CoGSS@CoCHNSs	**51.7**	**2.32**
$Mn_{(0.04)}$B-CoGSS@CoCHNSs	**61.3**	**3.84**

Table S2. Comparison of the overall water splitting data with some representative non-noble catalysts.

Catalysts	Electrolyte	Current density J (mA cm^{-2})	Cell voltage (V)	Reference
Fe_1Mn_1@BN-PCFs	**1 M KOH**	**10**	**1.62**	**[4]**
V_OB-Co_3O_4/NF	**1 M KOH**	**10**	**1.67**	**[5]**
FeCu@BNPCNS	**1 M KOH**	**10**	**1.613**	**[6]**
CoZnCdCuMnS@CF	**1 M KOH**	**10**	**1.63**	**[7]**
Co_1Mn_1CH/NF	**1 M KOH**	**10**	**1.68**	**[8]**
NiFe HNSs	**1 M KOH**	**10**	**1.67**	**[9]**
NiMn oxides	**1 M KOH**	**10**	**1.74**	**[10]**
Mn-CP NTs	**1 M KOH**	**10**	**1.67**	**[11]**
$Mn_{(0.04)}$B-CoGSS@CoCHNs	**1 M KOH**	**10**	**1.61**	**This work**

Table S3. Comparison of ORR activity data with some representative non-noble catalysts.

Catalyst	**Electrolyte**	**Half-wave potential (V)**	**Ref.**
MnCo–N–C	**0.1 M KOH**	**0.80**	**[12]**
Mn-Co_3O_4@CNTs	**0.1 M KOH**	**0.84**	**[13]**
$CoTe_2$/$MnTe_2$	**0.1 M KOH**	**0.81**	**[14]**
FeCo/NCNTs-800	**0.1 M KOH**	**0.87**	**[15]**
$Mn_{(0.04)}$B-CoGSS@CoCHNs	**0.1 M KOH**	**0.89**	**This work**

References

1 G. Li, Y. Tang, T. Fu, Y. Xiang, Z. Xiong, Y. Si, C. Guo and Z. Jiang, *Chem. Eng. J.*, 2022, **429**, 132174.

2 X. Xu, J. Xie, B. Liu, R. Wang, M. Liu, J. Zhang, J. Liu, Z. Cai and J. Zou, *Appl. Catal., B*, 2022, **316**, 121687.

3 A. Samanta, B. K. Barman, S. Mallick and C. R. Raj, *ACS Appl. Energy Mater.*, 2020, **3**, 10108.

4 Z. Liu, F. Guo, L. Cheng, X. Bo, T. Liu and M. Li, *J. Colloid Interface Sci.*, 2023, **629**, 179–192.

5 S. Bai, M. Yang, J. Jiang, X. He, J. Zou, Z. Xiong, G. Liao and S. Liu, *npj 2D Mater. Appl.*, 2021, **5**, 78.

6 N. Kumar T R, S. Kamalakannan, M. Prakash, B. Viswanathan and B. Neppolian, *ACS Appl. Energy Mater.*, 2022, **5**, 2104–2111.

7 Y. Lei, L. Zhang, W. Xu, C. Xiong, W. Chen, X. Xiang, B. Zhang and H. Shang, *Nano Res.*, 2022, **15**, 6054–6061.

8 T. Tang, W.-J. Jiang, S. Niu, N. Liu, H. Luo, Y.-Y. Chen, S.-F. Jin, F. Gao, L.-J. Wan and J.-S. Hu, *J. Am. Chem. Soc.*, 2017, **139**, 8320–8328.

9 X. Sun, Q. Shao, Y. Pi, J. Guo and X. Huang, *J. Mater. Chem. A*, 2017, **5**, 7769–7775.

10 M. Duraivel, S. Nagappan, J. Reddy, K. H. Park and K. Prabakar, *Electrochim. Acta*, 2023, **472**, 143372.

11 F. Tang, Y.-W. Zhao, Y. Ge, Y.-G. Sun, Y. Zhang, X.-L. Yang, A.-M. Cao, J.-H. Qiu and X.-J. Lin, *J. Colloid Interface Sci.*, 2022, **628**, 524–533.

12 G. Chao, Y. Zhang, L. Zhang, W. Zong, N. Zhang, T. Xue, W. Fan, T. Liu and Y. Xie, *J. Mater. Chem. A*, 2022, **10**, 5930–5936.

13 X. Zhang, Q. Liu, S. Liu and E. Wang, *Electrochim. Acta*, 2023, **437**, 141477.

14 Y. R. Rosyara, A. Muthurasu, K. Chhetri, I. Pathak, T. H. Ko, P. C. Lohani, D. Acharya, T. Kim, D. Lee and H. Y. Kim, *ACS Appl. Mater. Interfaces*, 2024, **16**, 10238–10250.

15 W. Zhang, Y.-P. Chen, L. Zhang, J.-J. Feng, X.-S. Li and A.-J. Wang, *J. Colloid Interface Sci.*, 2022, **626**, 653–661.